which is the Michaelis–Menten equation.

There are many other models of enzyme cooperativity, and the interested reader is referred to Dixon and Webb (1979) for a comprehensive discussion and comparison of other models in the literature.

1.3 Glycolysis and Glycolytic Oscillations

Metabolism is the process of extracting useful energy from chemical bonds. A metabolic pathway is the sequence of enzymatic reactions that take place in order to transfer chemical energy from one form to another. The common carrier of energy in the cell is the chemical *adenosine triphosphate* (ATP). ATP is formed by the addition of an inorganic phosphate group (HPO_4^{2-}) to *adenosine diphosphate* (ADP), or by the addition of two inorganic phosphate groups to *adenosine monophosphate* (AMP). The process of adding an inorganic phosphate group to a molecule is called *phosphorylation*. Since the three phosphate groups on ATP carry negative charges, considerable energy is required to overcome the natural repulsion of like-charged phosphates as additional groups are added to AMP. Thus, the hydrolysis (the cleavage of a bond by water) of ATP to ADP releases large amounts of energy.

Energy to perform chemical work is made available to the cell by the oxidation of glucose to carbon dioxide and water, with a net release of energy. Some of this energy is dissipated as heat, but fortunately, some of it is also stored in other chemical bonds. The overall chemical reaction for the oxidation of glucose can be written as

$$C_6H_{12}O_6 + 6O_2 \longrightarrow 6CO_2 + 6H_2O + \text{energy}, \tag{1.54}$$

but of course, this is not an elementary reaction. Instead, this reaction takes place in a series of enzymatic reactions, with three major reaction stages, *glycolysis*, the *Krebs cycle*, and the *electron transport* (or *cytochrome) system*.

Glycolysis involves 11 elementary reaction steps, each of which is an enzymatic reaction. Here we consider a simplified model of the initial steps. (To understand more of the labyrinthine complexity of glycolysis, interested readers are encouraged to consult a specialized book on biochemistry, such as Stryer, 1988.) The first three steps of glycolysis are (Fig. 1.4)

1. the phosphorylation of glucose to glucose 6-phosphate;
2. the isomerization of glucose 6-phosphate to fructose 6-phosphate; and
3. the phosphorylation of fructose 6-phosphate to fructose 1,6-bisphosphate.

This last reaction is catalyzed by the enzyme phosphofructokinase (PFK1).

PFK1 is an example of an allosteric enzyme as it is allosterically inhibited by ATP. Note that ATP is both a substrate of PFK1, binding at a catalytic site, and an allosteric inhibitor, binding at a regulatory site. The inhibition due to ATP is removed by AMP, and thus the activity of PFK1 increases as the ratio of ATP to AMP decreases. As PFK1 phosphorylates fructose 6-P, ATP is converted to ADP. ADP, in turn, is converted back

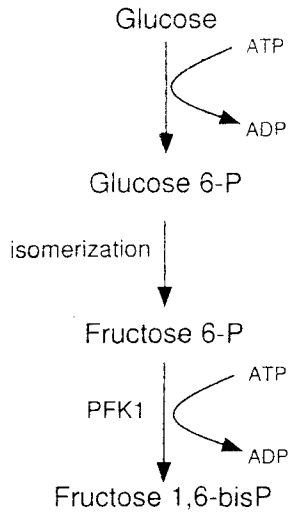

Figure 1.4 The first three reactions in the glycolytic pathway.

to ATP and AMP by the reaction

$$2\text{ADP} \rightleftharpoons \text{ATP} + \text{AMP},$$

which is catalyzed by the enzyme adenylate kinase. Since there is normally little AMP in cells, the conversion of ADP to ATP and AMP serves to significantly decrease the ATP/AMP ratio, thus activating PFK1. This is an example of a positive feedback loop; the greater the activity of PFK1, the lower the ATP/AMP ratio, thus further increasing PFK1 activity.

It was discovered in 1980 that in some cell types, another important allosteric activator of PFK1 is fructose 2,6-bisphosphate (Stryer, 1988), which is formed from fructose 6-phosphate in a reaction catalyzed by phosphofructokinase 2 (PFK2), a different enzyme from phosphofructokinase (PFK1) (you were given fair warning about the labyrinthine nature of this process!). Of particular significance is that an abundance of fructose 6-phosphate leads to a corresponding abundance of fructose 2,6-bisphosphate, and thus a corresponding increase in the activity of PFK1. This is an example of a negative feedback loop, where an increase in the substrate concentration leads to a greater rate of substrate reaction and consumption. Clearly, PFK1 activity is controlled by an intricate system of reactions, the collective behavior of which is not obvious a priori.

Under certain conditions the rate of glycolysis is known to be oscillatory, or even chaotic (Nielsen et al., 1997). This biochemical oscillator has been known and studied experimentally for some time. For example, Hess and Boiteux (1973) devised a flow reactor containing yeast cells into which a controlled amount of substrate (either glucose or fructose) was continuously added. They measured the pH and fluorescence of the reactants, thereby monitoring the glycolytic activity, and they found ranges of continuous input under which glycolysis was periodic.

A mathematical model describing this oscillation was proposed by Sel'kov (1968) and later modified by Goldbeter and Lefever (1972). It is meant to capture only the positive feedback of ADP on PFK1 activity, and does not take into account the negative feedback process that was discovered more recently. (An interesting exercise would be to construct a more detailed model, including both positive and negative feedback processes, to see what difference this makes to the conclusions.) In the Sel'kov model, PFK1 is inactive in its unbound state but is activated by binding with several ADP molecules. Note that, for simplicity, the model does not take into account the conversion of ADP to AMP and ATP, but assumes that ADP activates PFK1 directly, since the overall effect is similar. In the active state, the enzyme catalyzes the production of ADP from ATP as fructose-6-P is phosphorylated. Sel'kov's reaction scheme for this process is as follows: PFK1 (denoted by E) is activated or deactivated by binding or unbinding with γ molecules of ADP (denoted by S_2)

$$\gamma S_2 + E \underset{k_{-3}}{\overset{k_3}{\rightleftharpoons}} ES_2^\gamma,$$

and ATP (denoted S_1) can bind with the activated form of enzyme to produce a product molecule of ADP. In addition, there is assumed to be a steady supply rate of S_1, while product S_2 is irreversibly removed. Thus,

$$\xrightarrow{v_1} S_1, \tag{1.55}$$

$$S_1 + ES_2^\gamma \underset{k_{-1}}{\overset{k_1}{\rightleftharpoons}} S_1ES_2^\gamma \xrightarrow{k_2} ES_2^\gamma + S_2, \tag{1.56}$$

$$S_2 \xrightarrow{v_2}. \tag{1.57}$$

Applying the law of mass action to the Sel'kov kinetic scheme, we find five differential equations for the production of the five species $s_1 = [S_1], s_2 = [S_2], e = [E], x_1 = [ES_2^\gamma], x_2 = [S_1ES_2^\gamma]$:

$$\frac{ds_1}{dt} = v_1 - k_1 s_1 x_1 + k_{-1} x_2, \tag{1.58}$$

$$\frac{ds_2}{dt} = k_2 x_2 - k_3 s_2^\gamma e + k_{-3} x_1 - v_2 s_2, \tag{1.59}$$

$$\frac{dx_1}{dt} = -k_1 s_1 x_1 + (k_{-1} + k_2) x_2 + k_3 s_2^\gamma e - k_{-3} x_1, \tag{1.60}$$

$$\frac{dx_2}{dt} = k_1 s_1 x_1 - (k_{-1} + k_2) x_2. \tag{1.61}$$

The fifth differential equation is not necessary, because the total available enzyme is conserved, $e + x_1 + x_2 = e_0$. Now we introduce dimensionless variables $\sigma_1 = \frac{k_1 s_1}{k_2 + k_{-1}}$, $\sigma_2 = (\frac{k_3}{k_{-3}})^{1/\gamma} s_2$, $u_1 = x_1/e_0$, $u_2 = x_2/e_0$, $t = \frac{k_2 + k_{-1}}{e_0 k_1 k_2}\tau$ and find

$$\frac{d\sigma_1}{d\tau} = v - \frac{k_2 + k_{-1}}{k_2} u_1 \sigma_1 + \frac{k_{-1}}{k_2} u_2, \tag{1.62}$$

$$\frac{d\sigma_2}{d\tau} = \alpha\left[u_2 - \frac{k_{-3}}{k_2}\sigma_2^\gamma(1-u_1-u_2) + \frac{k_{-3}}{k_2}u_1\right] - \eta\sigma_2, \tag{1.63}$$

$$\epsilon\frac{du_1}{d\tau} = u_2 - \sigma_1 u_1 + \frac{k_{-3}}{k_2+k_{-1}}\left[\sigma_2^\gamma(1-u_1-u_2) - u_1\right], \tag{1.64}$$

$$\epsilon\frac{du_2}{d\tau} = \sigma_1 u_1 - u_2, \tag{1.65}$$

where $\epsilon = \frac{e_0 k_1 k_2}{(k_2+k_{-1})^2}$, $\nu = \frac{\nu_1}{k_2 e_0}$, $\eta = \frac{\nu_2(k_2+k_{-1})}{k_1 k_2 e_0}$, $\alpha = \frac{k_2+k_{-1}}{k_1}\left(\frac{k_3}{k_{-3}}\right)^{1/\gamma}$. If we assume that ϵ is a small number, then both u_1 and u_2 are "fast" variables and can be set to their quasi-steady values,

$$u_1 = \frac{\sigma_2^\gamma}{\sigma_2^\gamma\sigma_1 + \sigma_2^\gamma + 1}, \tag{1.66}$$

$$u_2 = \frac{\sigma_1\sigma_2^\gamma}{\sigma_2^\gamma\sigma_1 + \sigma_2^\gamma + 1} = f(\sigma_1, \sigma_2), \tag{1.67}$$

and with these quasi-steady values, the evolution of σ_1 and σ_2 is governed by

$$\frac{d\sigma_1}{d\tau} = \nu - f(\sigma_1, \sigma_2), \tag{1.68}$$

$$\frac{d\sigma_2}{d\tau} = \alpha f(\sigma_1, \sigma_2) - \eta\sigma_2. \tag{1.69}$$

The goal of the following analysis is to demonstrate that this system of equations has oscillatory solutions for some range of the supply rate ν. First observe that because of saturation, the function $f(\sigma_1, \sigma_2)$ is bounded by 1. Thus, if $\nu > 1$, the solutions of the differential equations are not bounded. For this reason we consider only $0 < \nu < 1$. The nullclines of the flow are given by the equations

$$\sigma_1 = \frac{\nu}{1-\nu}\frac{1+\sigma_2^\gamma}{\sigma_2^\gamma} \qquad \left(\frac{d\sigma_1}{d\tau} = 0\right), \tag{1.70}$$

$$\sigma_1 = \frac{1+\sigma_2^\gamma}{\sigma_2^{\gamma-1}(p-\sigma_2)} \qquad \left(\frac{d\sigma_2}{d\tau} = 0\right), \tag{1.71}$$

where $p = \alpha/\eta$. These two nullclines are shown plotted as dotted and dashed curves respectively in Fig. 1.5.

The steady-state solution is unique and satisfies

$$\sigma_2 = p\nu, \tag{1.72}$$

$$\sigma_1 = \frac{\nu(1+\sigma_2^\gamma)}{(1-\nu)\sigma_2^\gamma}. \tag{1.73}$$

The stability of the steady solution is found by linearizing the differential equations about the steady-state solution and examining the eigenvalues of the linearized system. The linearized system has the form

$$\frac{d\tilde{\sigma}_1}{d\tau} = -f_1\tilde{\sigma}_1 - f_2\tilde{\sigma}_2, \tag{1.74}$$

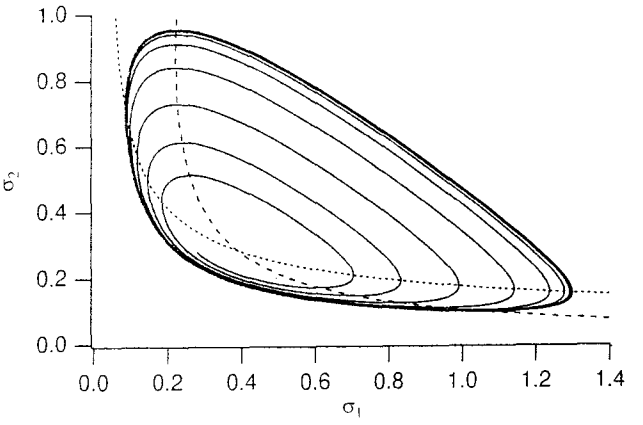

Figure 1.5 Phase portrait of the Sel'kov glycolysis system with $\nu = 0.0285, \eta = 0.1, \alpha = 1.0$, and $\gamma = 2$. Dotted curve: $\frac{d\sigma_1}{d\tau} = 0$. Dashed curve: $\frac{d\sigma_2}{d\tau} = 0$.

$$\frac{d\tilde{\sigma}_2}{d\tau} = \alpha f_1 \tilde{\sigma}_1 + (\alpha f_2 - \eta)\tilde{\sigma}_2, \tag{1.75}$$

where $f_j = \frac{\partial f}{\partial \sigma_j}, j = 1, 2$, evaluated at the steady-state solution, and where $\tilde{\sigma}_i$ denotes the deviation from the steady-state value of σ_i. The characteristic equation for the eigenvalues λ of the linear system (1.74)–(1.75) is

$$\lambda^2 - (\alpha f_2 - \eta - f_1)\lambda + f_1 \eta = 0. \tag{1.76}$$

Since f_1 is always positive, the stability of the linear system is determined by the sign of $H = \alpha f_2 - \eta - f_1$, being stable if $H < 0$ and unstable if $H > 0$. Changes of stability, if they exist, occur at $H = 0$, and are Hopf bifurcations to periodic solutions with approximate frequency $\omega = \sqrt{f_1 \eta}$.

The function $H(\nu)$ is given by

$$H(\nu) = \frac{(1 - \nu)}{(1 + y)}(\eta\gamma + (\nu - 1)y) - \eta, \tag{1.77}$$

$$y = (p\nu)^\gamma. \tag{1.78}$$

Clearly, $H(0) = \eta(\gamma - 1), H(1) = -\eta$, so for $\gamma > 1$, there must be at least one Hopf bifurcation point, below which the steady solution is unstable. Additional computations show that this Hopf bifurcation is supercritical, so that for ν slightly below the bifurcation point, there is a stable periodic orbit.

An example of this periodic orbit is shown in Fig. 1.5 with coefficients $\nu = 0.0285, \eta = 0.1, \alpha = 1.0$, and $\gamma = 2$. The evolution of σ_1 and σ_2 are shown plotted as functions of time in Fig. 1.6. This periodic orbit exists only in very small regions of parameter space, rapidly expanding until it contacts the $S_2 = 0$ axis, into which it collapses.

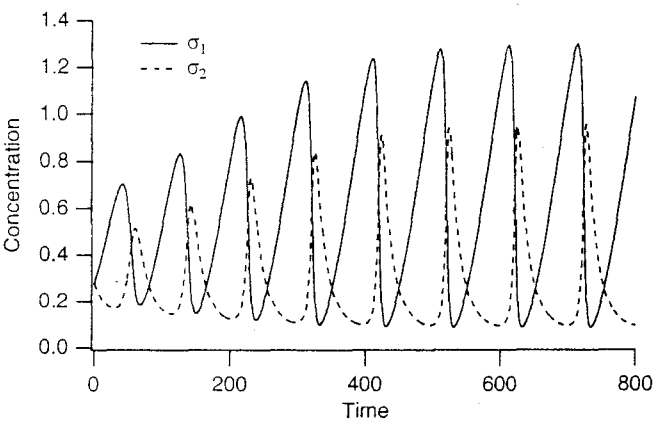

Figure 1.6 Evolution of σ_1 and σ_2 for the Sel'kov glycolysis system toward a periodic solution. Parameters are the same as in Fig. 1.5.

While the Sel'kov model has certain features that are qualitatively correct, it fails to agree with the experimental results at a number of points. Hess and Boiteux (1973) report that for high and low substrate injection rates, there is a stable steady-state solution. There are two Hopf bifurcation points, one at the flow rate of 20 mM/hr and another at 160 mM/hr. The period of oscillation at the low flow rate is about 8 minutes and decreases as a function of flow rate to about 3 minutes at the upper Hopf bifurcation point. In contrast, the Sel'kov model has but one Hopf bifurcation point.

To reproduce these additional experimental features we consider a more detailed model of the reaction. In 1972, Goldbeter and Lefever proposed a model of Monod–Wyman–Changeux type that provided a more accurate description of the oscillations. More recently, by fitting a simpler model to experimental data on PFK1 kinetics in skeletal muscle, Smolen (1995) has shown that this level of complexity is not necessary; his model assumes that PFK1 consists of four independent, identical subunits, and reproduces the observed oscillations well. Despite this, we consider only the Goldbeter–Lefever model in detail, as it provides an excellent example of the use of Monod–Wyman–Changeux models.

In the Goldbeter–Lefever model of the phosphorylation of fructose-6-P, the enzyme PFK1 is assumed to be a dimer that exists in two states, an active state R and an inactive state T. The substrate, S_1, can bind to both forms, but the product, S_2, which is an activator, or positive effector, of the enzyme, binds only to the active form. The enzymatic forms of R carrying substrate decompose irreversibly to yield the product ADP. In addition, substrate is supplied to the system at a constant rate, while product is removed at a rate proportional to its concentration. The reaction scheme for this is as follows: let T_j represent the inactive T form of the enzyme bound to j molecules of substrate and let R_{ij} represent the active form R of the enzyme bound to i substrate

molecules and j product molecules. Then

$$R_{00} \underset{k_{-1}}{\overset{k_1}{\rightleftharpoons}} T_0,$$

$$S_1 + R_{0j} \underset{k_{-2}}{\overset{2k_2}{\rightleftharpoons}} R_{1j} \xrightarrow{k} R_{0j} + S_2, \qquad S_1 + R_{1j} \underset{2k_{-2}}{\overset{k_2}{\rightleftharpoons}} R_{2j} \xrightarrow{2k} R_{1j} + S_2, \qquad j = 0, 1, 2,$$

$$S_2 + R_{00} \underset{k_{-2}}{\overset{2k_2}{\rightleftharpoons}} R_{01}, \qquad S_2 + R_{01} \underset{2k_{-2}}{\overset{k_2}{\rightleftharpoons}} R_{02},$$

$$S_1 + T_0 \underset{k_{-3}}{\overset{2k_3}{\rightleftharpoons}} T_1, \qquad S_1 + T_1 \underset{2k_{-3}}{\overset{k_3}{\rightleftharpoons}} T_2.$$

The possible receptor states are illustrated graphically in Fig. 1.7. In this system, the substrate S_1 holds the enzyme in the inactive state by binding with T_0 to produce T_1 and T_2, while product S_2 holds enzyme in the active state by binding with R_{00} to produce R_{01} and binding with R_{01} to produce R_{02}. There is a factor two in the rates of reaction because a dimer with two available binding sites reacts like twice the same amount of monomer.

The analysis of this reaction scheme is substantially more complicated than that of the Sel'kov scheme, although the idea is the same. We use the law of mass action to write differential equations for the fourteen chemical species. For example, the equation for

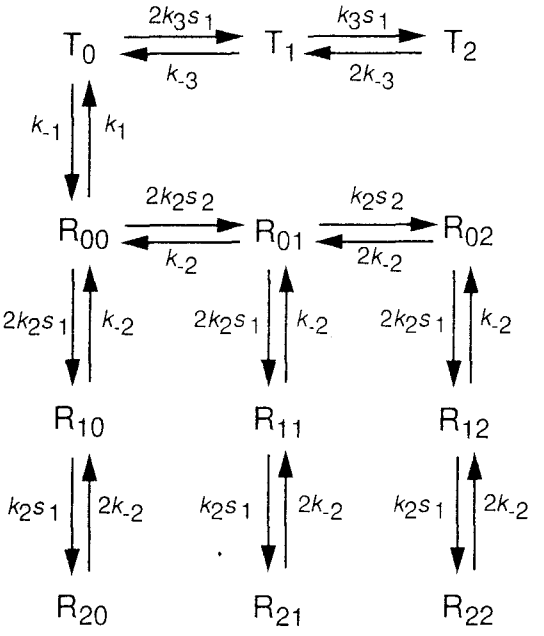

Figure 1.7 Possible receptor states of the Goldbeter–Lefever model for glycolytic oscillations.

$s_1 = [S_1]$ is

$$\frac{ds_1}{dt} = v_1 - F, \tag{1.79}$$

where

$$\begin{aligned} F = \; & k_{-2}(r_{10} + r_{11} + r_{12}) + 2k_{-2}(r_{20} + r_{21} + r_{22}) \\ & - 2k_2 s_1(r_{00} + r_{01} + r_{02}) - k_2 s_1(r_{10} + r_{11} + r_{12}) \\ & - 2k_3 s_1 t_0 - k_3 s_1 t_1 + k_{-3} t_1 + 2k_{-3} t_2, \end{aligned} \tag{1.80}$$

and the equation for $r_{00} = [R_{00}]$ is

$$\frac{dr_{00}}{dt} = -(k_1 + 2k_2 s_1 + 2k_2 s_2) r_{00} + (k_{-2} + k) r_{10} + k_{-2} r_{01} + k_{-1} t_0. \tag{1.81}$$

We then assume that all twelve of the intermediates are in quasi-steady state. This leads to a 12 by 12 linear system of equations, which, if we take the total amount of enzyme to be e_0, can be solved. We substitute this solution into the differential equations for s_1 and s_2 with the result that

$$\frac{ds_1}{dt} = v_1 - F(s_1, s_2), \tag{1.82}$$

$$\frac{ds_2}{dt} = F(s_1, s_2) - v_2 s_2, \tag{1.83}$$

where

$$F(s_1, s_2) = \left(\frac{2k_2 k_{-1} k e_0}{k + k_{-2}} \right) \left(\frac{s_1 (1 + \frac{k_2}{k + k_{-2}} s_1)(k_2 s_2 + k_{-2})^2}{k_{-2}^2 k_1 (\frac{k_3}{k_{-3}} s_1 + 1)^2 + k_{-1} (1 + \frac{k_2}{k + k_{-2}} s_1)^2 (k_{-2} + k_2 s_2)^2} \right). \tag{1.84}$$

Now we introduce dimensionless variables $\sigma_1 = \frac{k_2 s_1}{k_{-2}}, \sigma_2 = \frac{k_2 s_2}{k_{-2}}, t = \frac{\tau}{\tau_c}$ and parameters $\nu = \frac{k_2 v_1}{k_{-2} \tau_c}, \eta = \frac{v_2}{\tau_c}$, where $\tau_c = \frac{2k_2 k_{-1} k e_0}{k_1 (k + k_{-2})}$, and arrive at the system (1.68)–(1.69), but with a different function $f(\sigma_1, \sigma_2)$, and with $\alpha = 1$. If, in addition, we assume that

1. the substrate does not bind to the T form ($k_3 = 0$, T is completely inactive),
2. T_0 is preferred over R_{00} ($k_1 \gg k_{-1}$), and
3. if the substrate S_1 binds to the R form, then formation of product S_2 is preferred to dissociation ($k \gg k_{-2}$),

then we can simplify the equations substantially to obtain

$$f(\sigma_1, \sigma_2) = \sigma_1 (1 + \sigma_2)^2. \tag{1.85}$$

The nullclines for this system of equations are somewhat different from the Sel'kov system, being

$$\sigma_1 = \frac{\nu}{(1 + \sigma_2)^2} \qquad \left(\frac{d\sigma_1}{d\tau} = 0 \right), \tag{1.86}$$

$$\sigma_1 = \frac{\eta \sigma_2}{(1 + \sigma_2)^2} \qquad \left(\frac{d\sigma_2}{d\tau} = 0 \right), \tag{1.87}$$

and the unique steady-state solution is given by

$$\sigma_1 = \frac{\nu}{(1+\sigma_2)^2}, \tag{1.88}$$

$$\sigma_2 = \frac{\nu}{\eta}. \tag{1.89}$$

The stability of the steady-state solution is again determined by the characteristic equation (1.76), and the sign of the real part of the eigenvalues is the same as the sign of

$$H = f_2 - f_1 - \eta = 2\sigma_1(1+\sigma_2)^2 - (1+\sigma_2) - \eta \tag{1.90}$$

evaluated at the steady state (1.86)–(1.87). Equation (1.90) can be written as the cubic polynomial

$$\frac{1}{\eta}y^3 - y + 2 = 0, \qquad y = 1 + \frac{\nu}{\eta}. \tag{1.91}$$

For η sufficiently large, the polynomial (1.91) has two roots greater than 2, say, y_1 and y_2. Recall that ν is the nondimensional flow rate of substrate ATP. To make some correspondence with the experimental data, we assume that the flow rate ν is proportional to the experimental supply rate of glucose. This is not strictly correct, although ATP is produced at about the same rate that glucose is supplied. Accepting this caveat, we see that to match experimental data, we require

$$\frac{y_2 - 1}{y_1 - 1} = \frac{\nu_2}{\nu_1} = \frac{160}{20} = 8. \tag{1.92}$$

Requiring (1.91) to hold at y_1 and y_2 and requiring (1.92) to hold as well, we find numerical values

$$y_1 = 2.08, y_2 = 9.61, \eta = 116.7 \tag{1.93}$$

corresponding to $\nu_1 = 126$ and $\nu_2 = 1005$.

At the Hopf bifurcation point, the period of oscillation is

$$T_i = \frac{2\pi}{\omega_i} = \frac{2\pi}{\sqrt{\eta}(1+\sigma_2)} = \frac{2\pi}{\sqrt{\eta}y_i}. \tag{1.94}$$

For the numbers (1.93), we obtain a ratio of periods $T_1/T_2 = 4.6$, which is acceptably close to the experimentally observed ratio $T_1/T_2 = 2.7$.

A typical phase portrait for the periodic solution that exists between the Hopf bifurcation points is shown in Fig. 1.8, and the concentrations of the two species are shown as functions of time in Fig. 1.9.

1.4 Appendix: Math Background

It is certain that some of the mathematical concepts and tools that we routinely invoke here are not familiar to all of our readers. In this first chapter alone, we have